Smart Grid and Renewable Energy, 2024, 15, 107-122
https://www.scirp.org/journal/sgre
ISSN Online: 2151-4844
ISSN Print: 2151-481X

Performance Evaluation of Solar Chimney Draft: Application to Ventilation

Boukaré Ouedraogo[1,2*], Adama Ouedraogo[1,3], Arouna Kabore[1], Kalifa Palm[1,4], Dieudonné Joseph Bahiebo[1]

[1]Laboratoire d'Energies Thermiques Renouvelables (LETRE), Université Joseph KI-ZERBO: UFR/SEA, Ouagadougou, Burkina Faso
[2]Laboratoire de Chimie Analytique, Physique Spatiale et Energétique (LACAPSE), Université Norbert ZONGO, Koudougou, Burkina Faso
[3]Centre Universitaire Polytechnique de Kaya (CUP-Kaya), Université Joseph KI-ZERBO, Ouagadougou, Burkina Faso
[4]Laboratoire des Systèmes d'Energie Renouvelable et Environnement, Institut de Recherche en Sciences Appliquées et Technologies (IRSAT), Centre National de la Recherche Scientifique et Technologique (CNRST), Ouagadougou, Burkina Faso
Email: *boubakont2015@gmail.com

How to cite this paper: Ouedraogo, B., Ouedraogo, A., Kabore, A., Palm, K. and Bahiebo, D.J. (2024) Performance Evaluation of Solar Chimney Draft: Application to Ventilation. *Smart Grid and Renewable Energy*, **15**, 107-122.
https://doi.org/10.4236/sgre.2024.154007

Received: March 16, 2024
Accepted: April 27, 2024
Published: April 30, 2024

Abstract

Ventilation is one of the factors contributing to energy consumption in buildings and food preservation. The solar chimney proves to be an alternative for reducing conventional energy consumption. Thus, in this study, the performance of a solar chimney with two active faces for thermally drawing air from a chamber for preserving agri-food products was evaluated. These performances were experimentally assessed through data measurements: temperatures and velocities within the chimney, and their analysis using Excel and MATLAB. The obtained results were compared with those from literature to verify their validity. From this study, it is found that the maximum temperature at the chimney outlet reaches 49.4˚C with an average value of 43.7˚C. Additionally, the heating evolution of the chimney air presents four (04) identical phases in pairs, reflecting the chimney's operation throughout day. The temperature difference between the outlet and inlet of the chimney reaches a maximum of 17˚C with an average of 12.6˚C. Regarding airflow, the maximum air velocity at the chimney outlet is 0.8 m/s, and the average velocities have consistently been greater than or equal to 0.46 m/s. Thus, it can be concluded that the solar chimney is capable of providing ventilation for the preservation chamber through thermal draft.

Keywords

Solar Chimney, Natural Ventilation, Thermal Draft, Airflow, Chimney Effect

1. Introduction

Ventilation based on thermal buoyancy-driven draft has been extensively studied as a fundamental role in natural ventilation techniques. By harnessing the potential of solar radiation, passive solar design strategy could serve multiple functions in reducing energy consumption [1] [2]. According to the airflow model, passive ventilation systems can achieve natural ventilation [3] [4], heating [5], cooling [6] [7] of spaces, and preheating of air [8]. For ventilation, several types or configurations of solar chimneys exist. Depending on the configuration, these include trombe wall solar chimneys, roof solar chimneys [9] [10] [11], vertical solar chimneys [12] [13], as well as inclined solar chimneys [14] [15], and solar tower chimneys. Solar tower chimneys are typically used for electricity generation.

In order to enhance the performance of solar chimneys, numerous studies have been conducted addressing several parameters including chimney height, hydraulic diameter or dynamic vein, height-to-hydraulic diameter ratio, and inclination angle, among others. Typical values for the height of passive solar chimneys range from 1 m to 6 m [16] [17] [18] [19] [20]. However, exceptionally tall passive solar chimneys have been encountered, with heights reaching up to 21 m [21].

For instance, a solar wall chimney measuring 4 m in height and with an air section of 0.025 m^2, subjected to a flux of 400 W/m^2 [22], numerically obtained an average outlet temperature of 43˚C and a mass flow rate of air extraction of 0.014 kg/s. For the same flux, but a solar wall chimney measuring 2 m in height and with a flow diameter of 14.5 cm, [23] found an average outlet air temperature of 40˚C and a mass flow rate ranging from 0.016 to 0.018 kg/s.

With a 1 m tall solar wall chimney, [24] experimentally and theoretically demonstrated that the air velocity at the outlet can reach 0.24 m/s for a flow diameter of 0.332 m and an air inlet diameter of 0.13 m when the flux reaches 700 W/m^2.

In a numerical study using Computational Fluid Dynamics (CFD) [25], it was shown that beyond 0.2 m, the influence of hydraulic diameter on mass flow rate is negligible. Additionally, [26] addressed vertical solar chimneys by studying the influence of the ratio of hydraulic diameter to height (b/L). They showed that for asymmetric heating of plates, beyond 0.2, the b/L shape ratio has almost no influence on the Nusselt number. This implies that the thermal effect becomes negligible beyond $b/L = 0.2$.

Furthermore, [27] conducted a numerical study on the effect of the ratio of hydraulic diameter to height on the maximum heat transfer rate in the case of asymmetric heating. They found that the optimum shape ratio is 0.198, 0.117, 0.069, and 0.040 respectively for $R_{aL} = 10^5, 10^6, 10^7, 10^8$. This allowed the authors to show that for $10^5 \le R_{aL} \le 10^7$, the correlative relationship giving the optimum shape ratio is $(b/L)_{opt} = 2.8(R_{aL})^{-0.23}$.

Inclined solar chimneys, like roof solar chimneys, share the common characteristic of being inclined. However, their distinction lies in how they are integrated into the ventilated enclosure. If the chimney is part of the roof, a section of the roof, or a component of the roof, it is called a roof chimney [28]. But when the chimney integrates into the enclosure without depending on the roof but is inclined, it is called an inclined chimney [11]. With the inclination, the solar collector of the chimney receives more radiant power. This has sparked interest among many researchers such as [29]. They investigated a 50˚ inclined solar chimney relative to the horizontal. It has a height of 1 m and a hydraulic diameter of 0.15 m. The results show that the best performance is a flow rate of 0.040 kg/sec and an air renewal rate per hour of 157 when the radiation is 820 W/m^2.

[30] experimentally and numerically studied a 2 m long solar chimney with a dynamic vein of 5 cm. Its inclination angle varies from 15˚ to 60˚. When the heat flux varies from 150 W/m^2 to 750 W/m^2 for an inclination of 60˚, the volumetric flow rate ranges from 50 to 425 m^3/h. The fluid flow velocity ranges from 0.3 to 0.79 m/s at the outlet of the 5 cm thick dynamic vein.

Moreover, aiming to find the optimum inclination angle, [14] used experimental and theoretical methods to study the effect of the inclination angle of the solar chimney on the ventilation rate during the summer period. A roof solar chimney with a surface area of 1 m^2, inclined at 45˚C with an airflow section of 0.35 m^2. The theoretical and experimental results are consistent and show that the optimum inclination is between 45˚ and 60˚ depending on the altitude.

As for [31], they studied a solar chimney inclined at 60˚ relative to the horizontal, with a length of 1.5 m, a width of 0.75 m, and a hydraulic diameter of 0.2 m. Similarly, [32] examined the thermal performance of a passive cooling system by an inclined roof solar chimney at a 45˚ angle.

Regardless of the type of chimney, the common physical principle is that air density gradients primarily produce pressure differences at various locations [33]. Therefore, energy is required to induce these density gradients and create pressure differences. The chimney thus assumes this precise role by providing the necessary energy through the conversion of solar radiation into heat, which it transfers to the fluid (air) to induce its upward movement by buoyancy. Thus, it is essential to ensure the existence of solar potential. Burkina Faso is a Sahelian country with a high insolation potential and a solar energy potential of 5.5 kWh/m^2 per day [34]. The solar chimney, as a passive ventilation technology, is therefore a viable solution in Burkina Faso. However, solar chimneys are not currently utilized in Burkina Faso.

In the scientific literature, the solar chimneys discussed, whether inclined, vertical, or of the roof and Trombe wall type, typically have a single active face. Additionally, solar chimneys are generally used in residential settings. Therefore, to add to the existing array of chimneys while aiming to improve their performance, a study on the performance evaluation of a vertical solar chimney with two active faces is proposed.

2. Experimental Method

2.1. Solar Chimney

The solar chimney was initially designed using Autocad before its construction, as illustrated in Figure 1. It is 3 meters long and 2 meters high. It consists of two thermal solar collectors on its East and West faces, spaced 0.5 meters apart, which is the hydraulic diameter or the thickness of the dynamic vein.

The chimney on its active faces is oriented East-West and couples with a conservation chamber whose door and two windows are on the south face. It has three ventilation holes measuring 0.35 × 0.15 m^2 on each of the East and West faces.

For construction, a parallelepiped mesh of 3 × 2 × 0.5 m^3 is made using 5 IPN iron bars (see Figure 2(a)). Plywood sheets are placed on the 2 × 0.5 m^2 faces (South and North sides). Then, mild steel sheets are placed on the 3 × 2 m^2 faces (East and West sides) (see Figure 2(b) and Figure 2(c)). Clear glass sheets of 5mm are then placed on these same faces (see Figure 2(d)). The steel sheets and glass are separated by 5 cm of inert air. A hood is installed above to limit dust and protect against rain (see Figure 2(e)). The South and North faces are the inactive sides made of 5mm plywood painted in black (see Figure 2(e)). Thus, a solar chimney with a 3 × 0.5 m^2 air extraction section was constructed. Figure 3 describes the different elements

Figure 1. Designing model.

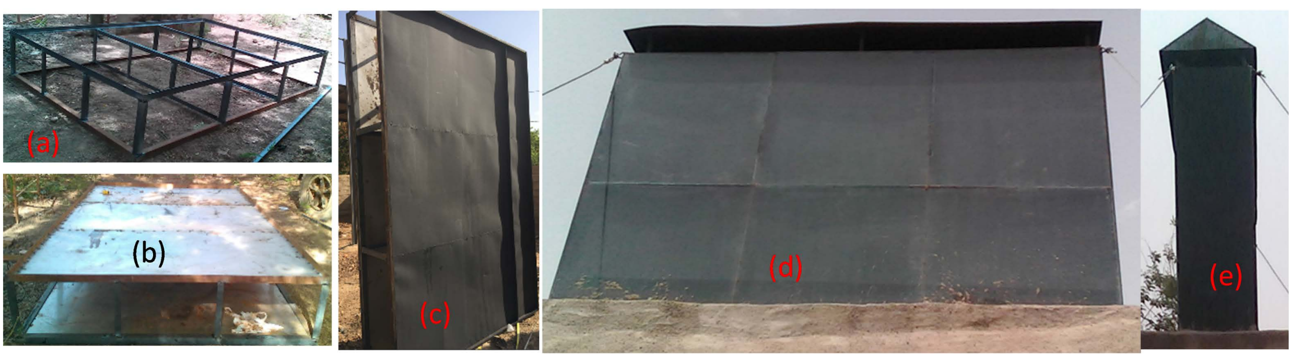

Figure 2. Steps of chimney construction (a) mesh, (b) placement of the absorber, (c) chimney painted black, (d) installation of the glass, and attachment of the hood (e).

and environments constituting the solar chimney.

2.2. Data Acquisition and Processing

The parameters involved are: temperature, air flow velocity, and solar radiation density. Temperatures at the inlet and outlet of the chimney were measured using type K thermocouples via a data logger. Solar radiation is measured using a second-class SR03 pyranometer and presented by [35]. The air velocity at the chimney outlet is deduced using Equation (1). The operating principle is as follows: solar radiation captured by the collector heats the air in the dynamic vein which sees its temperature increased and generates buoyancy (**Figure 4**). At the inlet the air is less hot (blue arrow) and hotter at the outlet (red arrow). Temperatures are measured at the inlet and outlet at three points aligned along the

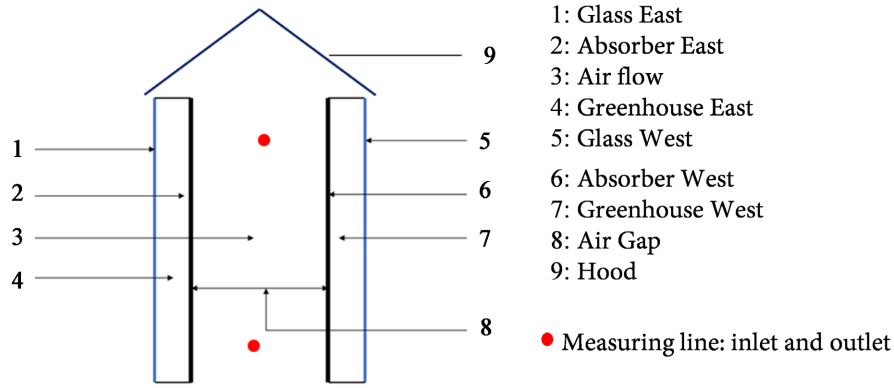

Figure 3. Constituent elements of the solar chimney and temperature measurement line

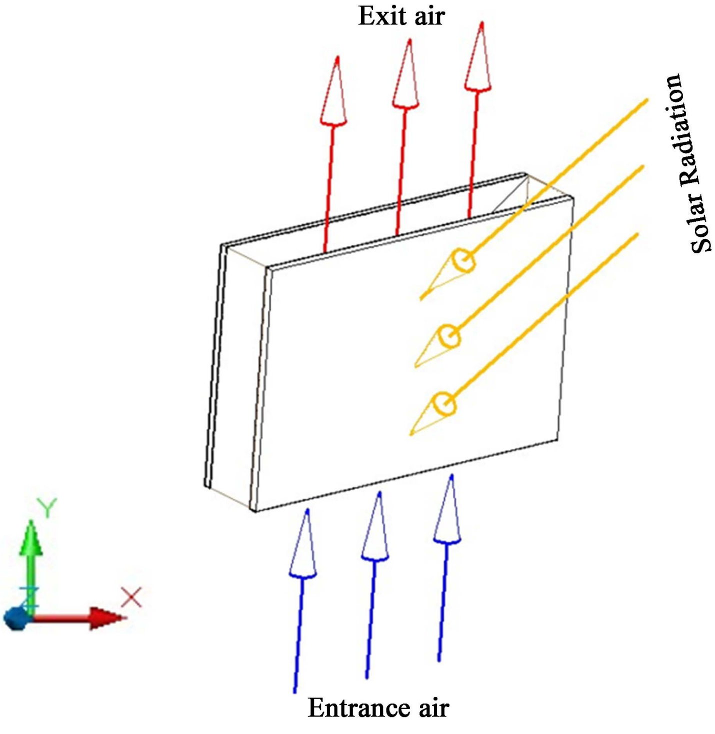

Figure 4. Operation of thermal draft.

length of the chimney. The average of the three inlet temperatures gives the inlet temperature and the average of the three at the outlet is the outlet temperature (**Figure 3**).

These data were then processed using Excel and MATLAB, specifically for deducing the velocity.

The air extraction capacity of the chimney is evaluated using parameters such as velocity or air flow rate at its outlet. This can be achieved using a fine anemometer, as the velocities are relatively low, or by evaluating the temperature difference between the chimney outlet and inlet, and then deducing the velocity according to the formula [36]:

$$v = \frac{\sqrt{2\beta g \Delta T \times \Delta H}}{\sqrt{\left(K_{\text{int}}\left(\frac{A_{ext}}{A_{\text{int}}}\right) + K_{ext} + f_{ext}\frac{H}{D_h}\right)}} \quad (1)$$

A_{ext} and A_{int} : are respectively the outlet and inlet sections of the chimney.

β : is the coefficient of thermal expansion.

ΔH: is the difference in altitude between the air outlet and inlet.

ΔT: is the temperature difference between the chimney outlet and inlet.

g: is the acceleration due to gravity.

K_{ext} and K_{int}: are respectively the pressure loss coefficients at the chimney outlet and inlet.

f_{ext} : is the friction factor of the chimney walls (absorbers).

D_h: is the hydraulic diameter.

H: is the height of the chimney.

According to [37] [38], typical constant values are: $K_{ext} = 1.5$, $K_{\text{int}} = 1.0$, $f_{ext} = 0.056$.

As a fine anemometer was not available, this formula was used for deducing the velocity. The application of this formula is straightforward: experimentally determine the difference between the temperature at the outlet and the temperature at the inlet of the chimney. Knowing the temperature of the air in the middle of the chimney, deduce the coefficient of thermal expansion. With the other terms being constants, a small calculation program allows the determination of the fluid velocity at the chimney outlet over time.

3. Results and Discussions

3.1. Heating of Draft Air: Chimney Outlet-Inlet Temperature Gap

The solar chimney's ability to draw air is dependent on its heating power of the air in its flow channel. The warmer the air, the less dense it becomes, resulting in higher flow velocity. Therefore, it is crucial to study the behavior of air temperature at the inlet and outlet of the chimney to determine its ability to provide the necessary heat for raising the air temperature in its dynamic vein. This allows for the evaluation of the chimney's performance as thermal draft technology.

It is observed that the maximum temperatures reached are 49.4˚C (**Figure 5**) and 48.9˚C (**Figure 6**) between 3:00 PM and 3:45 PM. This might lead one to believe that this is the time interval during which the chimney receives the most solar flux. However, this is not exactly the case. It is because during this period, the heat output from both the East and West absorbers is at its maximum. Indeed, each face of the chimney has its peak received flux, with that of the East face occurring around 10:00 AM to 11:30 AM depending on the time of year, and that of the West face observed around 2 PM to 3:45 PM, also depending on the month of the year. However, before noon, there is not observed a peak in fluid temperature of the same magnitude as in the afternoon, because the heat emitted by the East absorber is used to heat the fluid and the West absorber, which does not receive solar radiation during this period.

Figures 7-9 depict the evolution of the difference: outlet temperature—inlet temperature of the chimney. It reaches a maximum of 17.2˚C and 12.6˚C. This evolution presents four (04) phases reflecting the chimney's operation throughout the day. Phase 1: It is a rising phase that is limited to around 10:30 AM -

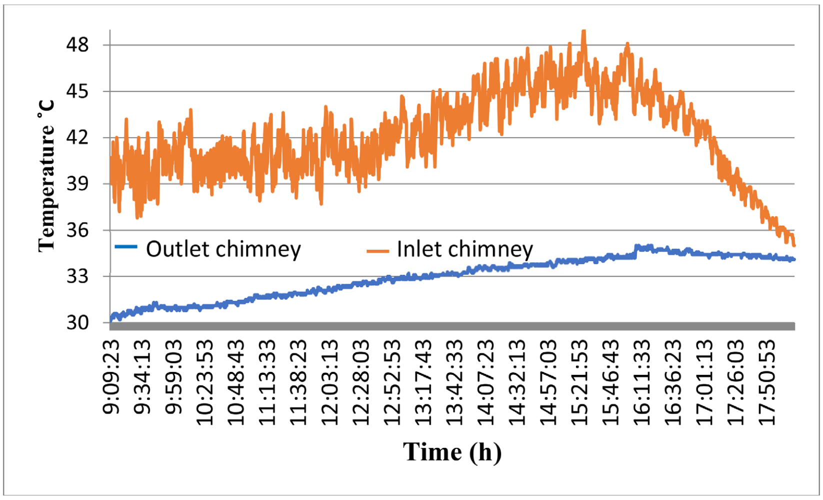

Figure 5. Variation of temperatures at the entrance and exit of the chimney 1st test.

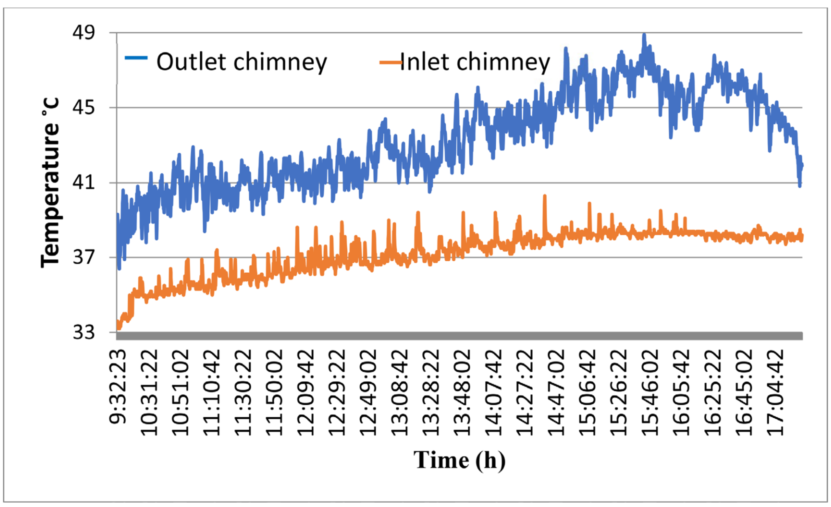

Figure 6. Evolution of temperatures at the entrance and exit of the chimney 2nd test.

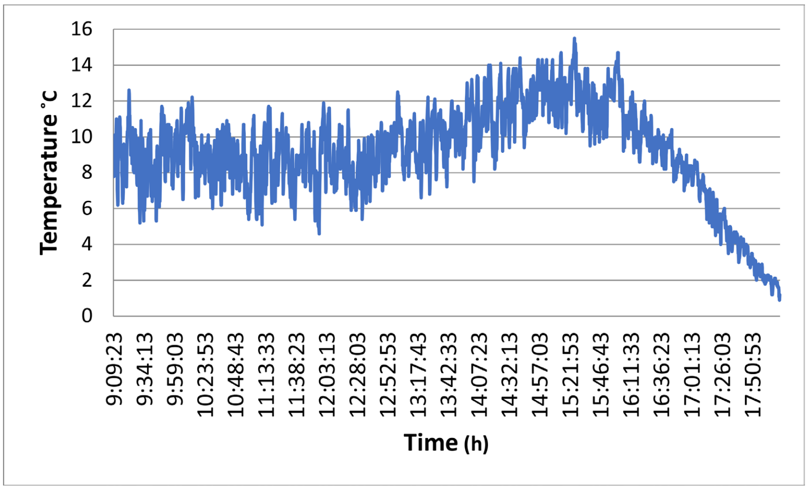

Figure 7. Evolution of the difference between the temperature at the outlet and at the inlet of the chimney 1st test.

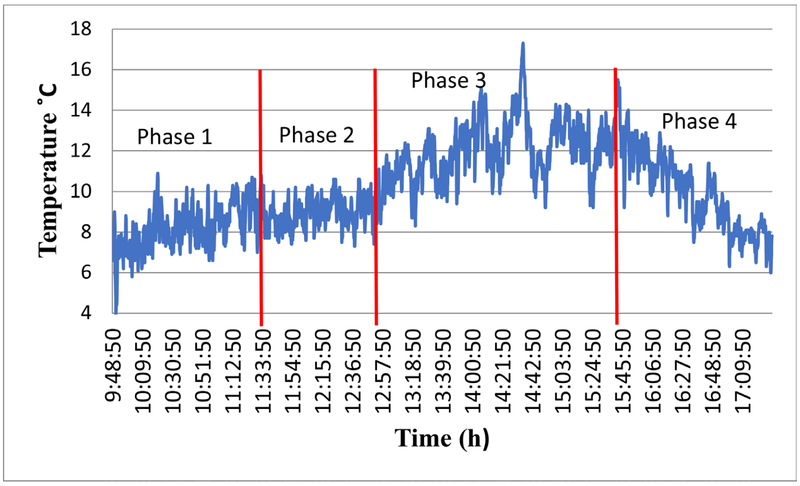

Figure 8. Evolution of the difference between the temperature at the outlet and at the inlet of the chimney 2nd test.

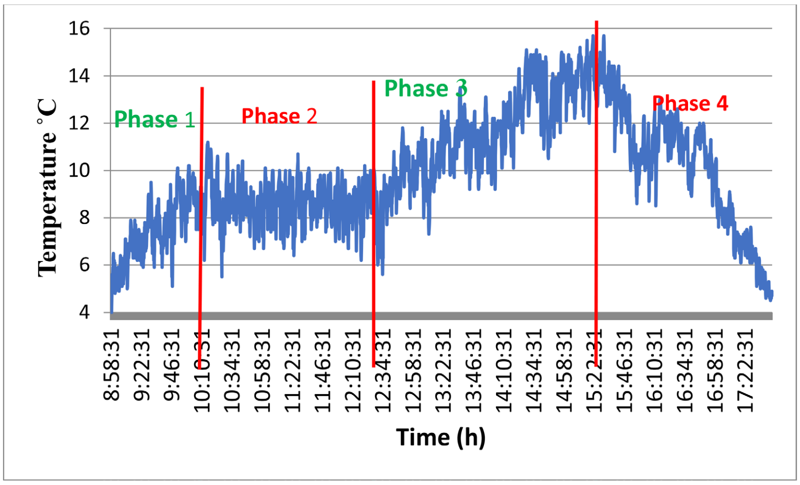

Figure 9. Evolution of the difference between the temperature at the outlet and the inlet of the chimney 3rd test.

11:30 AM. It corresponds to the period of fluid (air) warming by the East absorber: the chimney effect increases. Phase 2: It is descending, forming a convex inflection. It ranges from 11:30 AM to 1:00 PM. This period coincides with the sun's passage to a position where its rays tend to be parallel to the vertical on the horizontal plane. As a result, neither the East nor West thermal sensors receive them fully. This leads to their cooling and consequently the decrease in the temperature of the flowing fluid: the chimney effect decreases. Phase 3: An ascending phase admitting a concave inflection, indicating the next decreasing phase. It generally covers the period from 1:00 PM to 4:00 PM at the maximum, depending on the month of the year. It clearly indicates that the difference in temperature at the outlet—temperature at the inlet of the chimney increases. This means that the East and West absorbers release the maximum calories to the flowing fluid: the chimney effect is predominant. Phase 4: It corresponds to a period when solar radiation diminishes. Thus, the thermal sensors cool down, and the temperature of the fluid at the outlet decreases. As a result, the difference between the chimney outlet temperature and the inlet temperature decreases. This indicates that the effect of thermal draft decreases.

3.2. Influence of the External Ambience

Through **Figure10**, it is observed that the maximum temperature at the outlet is 46.5˚C at 2:36 PM. Meanwhile, the ambient temperature is 38˚C at 2:34 PM, and the illumination is 930W/m² at 11:54 AM. Similarly, for **Figure 11**, the maximum radiation of 893W/m² is reached at 12:02 PM, the maximum outlet temperature of 45˚C is obtained at 3:22 PM, with an ambient temperature of 37.3˚C at 3:18 PM. From this analysis, it is clear that the effect of the external environment on the fluid temperature is predominant. The fluid temperature at the chimney outlet increases with the external ambient temperature. However, the opposite is observed with the solar radiation received on a horizontal plane. This

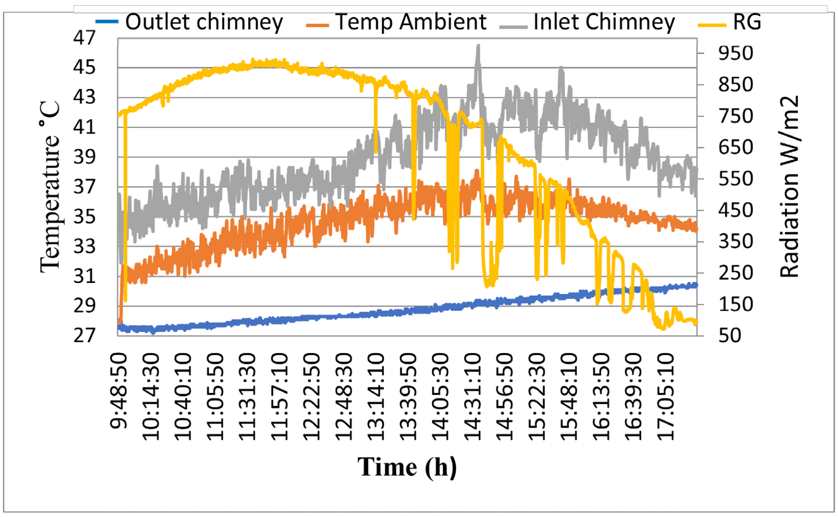

Figure 10. Effect of the external environment on the temperatures at the inlet and outlet of the chimney 1st test.

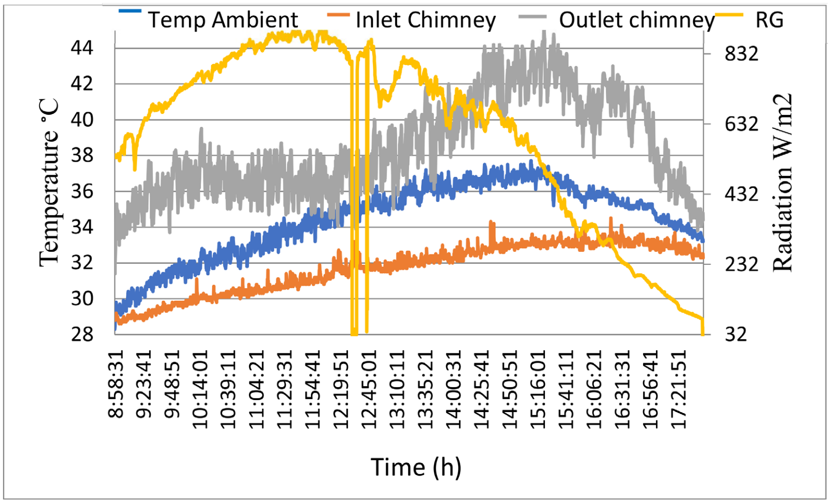

Figure 11. Effect of the external environment on the temperatures at the inlet and outlet of the chimney 2nd test.

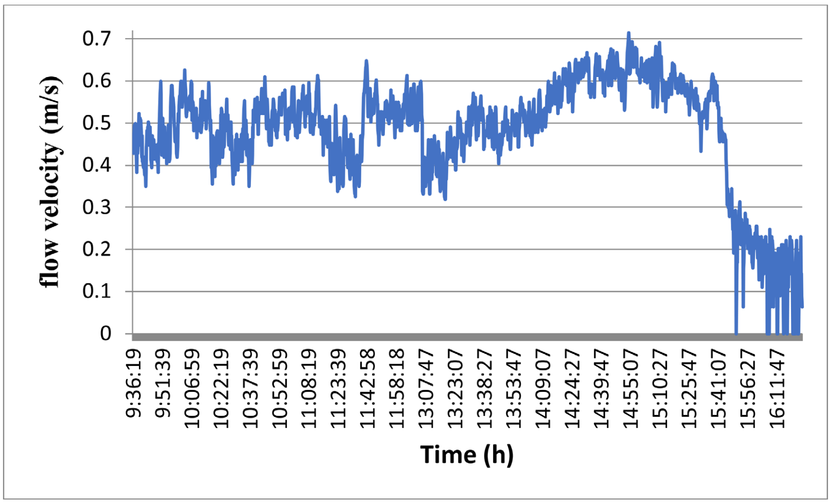

Figure 12. Variation in air speed at the chimney outlet 1st test.

is because the transmission of the received flux to the surface of the glass, then to the absorber, and from the absorber to the air creates a time lag.

3.3. Thermal Draft: Air Speed at the Chimney Outlet

The thermal draft of air is characterized by the velocity at the chimney outlet and is represented in **Figures 12-15**. The maximum air velocity is 0.8 m/s, attained between 2:00 PM and 3:30 PM (**Figure 14** and **Figure 15**). [30] obtained experimentally under similar climatic conditions (hot and dry) a slightly lower value (0.7 m/s) but with a chimney of dimensions 2 × 2 × 0.05 m^3 and inclined at an angle of 60˚. For all measurements taken, the average velocities have consistently been greater than or equal to 0.46 m/s. This is more than sufficient to ensure air renewal in the storage chamber, which required a minimum velocity of 0.062 m/s for adequate renewal.

We see a slight growth with a peak (0.67m/s for **Figure 14** 0.64 m/s for **Figure 12**

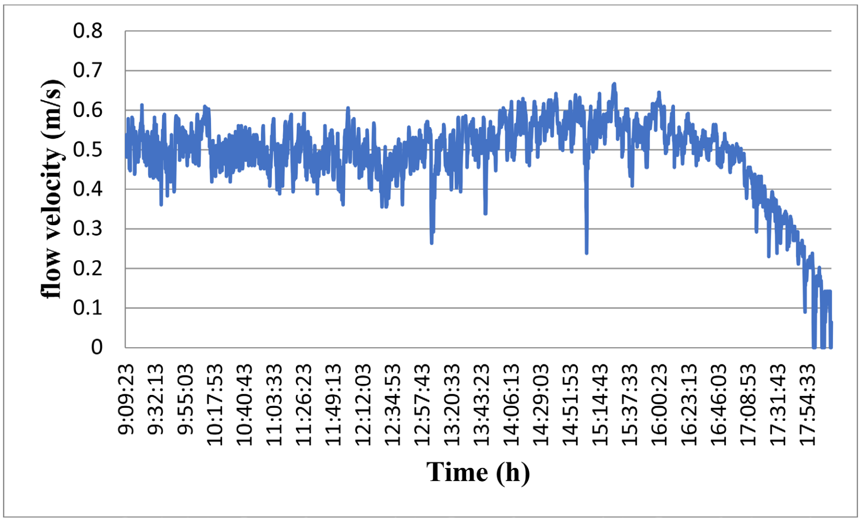

Figure 13. Variation in air speed at the chimney outlet 2nd test.

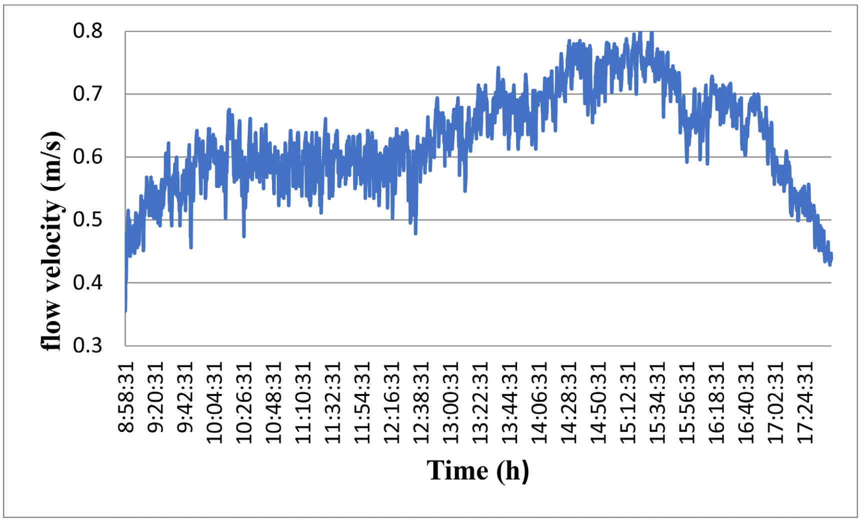

Figure 14. Variation in air speed at the chimney outlet 3rd test.

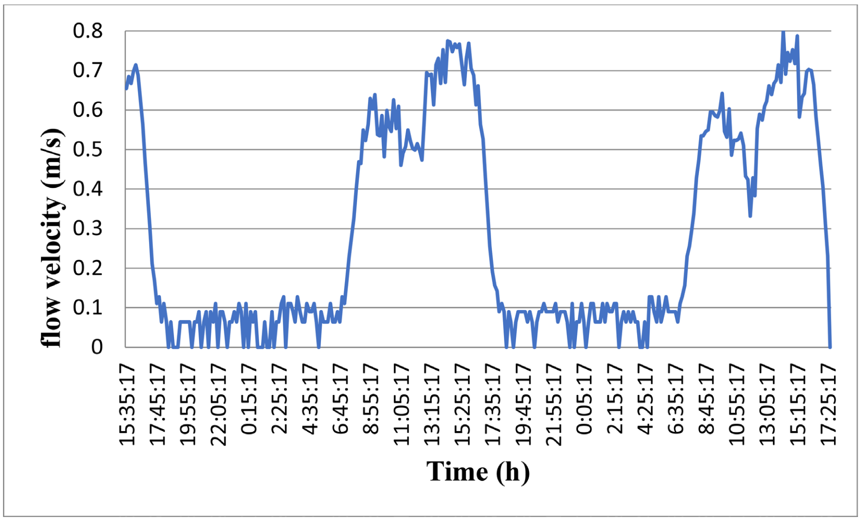

Figure 15. Variation in air speed at the chimney outlet for two full days.

and **Figure 15**), between 10:30 a.m. to 11:30 a.m. and a second peak (0.7 m/s in **Figure 10**, 0.8 m/s for **Figure 14** and **Figure 15**) greatest between 2:30 p.m. and 3:30 p.m. This is due to the effect of the two active East – West faces of the chimney. Otherwise we should observe a single peak in the interval around 10:30 a.m. and 11:30 a.m., given the chimney is vertical.

3.4. Validation of Results

We aim to compare our experimental results with those reported in the literature for validation purposes.

We remind that the solar chimney is 3 m long, 2 m high, and has a duct of 0.5 m. The experiments conducted here on the vertical chimney have shown that the maximum air temperatures at the thermosiphon outlet range from 48.9˚C **Figure 5**) to 49.4˚C (**Figure 6**).

However, with an inclined solar chimney of 45˚ and dimensions of 1 × 1 × 0.18 (length × width × dynamic vein) [28], the experimental temperature of the air at the outlet was found to be 55˚C. The noted difference between their result and ours is certainly due to the inclination of their chimney, which allows for maximum solar radiation capture. Additionally, their chimney's duct is smaller, resulting in less air volume to heat.

Meanwhile, [16] found that the air temperature at the outlet of a vertical chimney is 60˚C near the hot wall and 40˚C near the cold wall, averaging approximately 50˚C at the center of the channel for H = 23.1 MJ/m^2 and T_{amb} = 28.9˚C. Thus, on average, this result is consistent with our experiment.

Another principal performance parameter of the thermosiphon is the air velocity at its outlet or the volumetric or mass flow rate. Experimentally, we found a maximum air velocity of 0.8 m/s (**Figure 15**). While [30] obtained experimentally under similar climatic conditions (hot and dry) a slightly lower value (0.7 m/s) but with a chimney of dimensions 2 × 2 × 0.05 m^3 and inclined at an angle of 60˚. [20] obtained a similar result (a maximum air flow rate of 374 m^3/h, equivalent to 0.69 m/s when solar flux is 604 W/m^2) with a vertical chimney measuring 4.5 m in height, 1 m in width, and 0.15 m in diameter with a black-painted concrete absorber. These results are close to those of our work even though the dimensions and models are not exactly the same.

Theoretically, authors such as [39] observed a maximum velocity of 0.7 m/s at the outlet when both hot walls are at 60˚C, for a vertical solar chimney with a height of 1.5 m and an air duct of 0.2 m.

Similarly, with a solar chimney having a 0.23 m air duct, 6.5 m in height, and 1.64 m in length, [19] obtained 0.8 m/s, corresponding to a volume flow rate of 0.161 m^3/s in the 0.2 m duct and 0.43 m/s, corresponding to a flow rate of 0.238 m^3/s in the 0.55 m duct for a flux of 300 W/m^2.

For a vertical solar chimney with a height of 2 m and a 0.05 m gap at a hot wall temperature of 45˚C, [40] obtained 0.5 m/s and 35˚C, respectively, for the air velocity and temperature at the chimney outlet.

All these results are in agreement with the experimental values found in this study. The significant difference observed between the values (0.8 m/s and 49.4˚C) and those of [40] (0.5 m/s and 35˚C) is simply due to the low temperature (45˚C) of the hot walls of their chimney.

4. Conclusions and Perspectives

At the end of this study evaluating the thermal draft performance of a solar chimney, it is clear that the solar chimney assumes the natural ventilation of the storage chamber. This is evidenced by the results:

- The maximum temperatures reached are 49.4˚C and 48.9˚C between 3:00 PM and 3:45 PM. The average temperature at the chimney outlet is 43.7˚C.
- The evolution of the temperature of the air heated by the chimney can be divided into four distinct phases, reflecting the operation of the chimney over a full day. These phases are as follows: two increasing temperature phases occur from the morning until 11:30 AM and from 1:00 PM to 4:00 PM, with variations depending on the month of the year; and two decreasing temperature phases occur between 11:30 AM and 1:00 PM, as well as after 4:00 PM.
- The temperature difference between the chimney outlet and inlet reaches a maximum of 17˚C with an average of 12.6˚C.
- For draft, the maximum air velocity is 0.8 m/s, obtained between 2:00 PM and 3:30 PM.
- The average velocities have always been greater than or equal to 0.46 m/s. This is more than sufficient to ensure air renewal in the storage chamber, which requires at least a velocity of 0.062 m/s for renewal.

However, these performances could improve if the chimney outlet were redone by narrowing the outlet section to optimize the flow at this level. In this way, the hood could only be adjusted to this outlet and avoid the effect of its shading on the chimney and promote flow at the outlet.

Considering the chimney outlet temperature does not exceed 50˚C, the chimney could be tested for versatile use in drying edible leaves such as moringa, Rumex, L'*Hibiscus sabdariffa* (*oseille*), Adansonia digitata (baobab), etc. Indeed, the chimney studied in this work is intended for ventilating a chamber for storing onion bulbs, and storage is not continuous throughout the year. Therefore, the chimney could be used for other purposes during non-storage periods.

Acknowledgements

The authors gratefully acknowledge the International Science Program (ISP) for supporting BUF01 in Burkina Faso.

Conflicts of Interest

The authors declare no conflicts of interest regarding the publication of this paper.

References

[1] Noorollahi, Y., Golshanfard, A., Ansaripour, S., Khaledi, A. and Shadi, M. (2021)

Solar Energy for Sustainable Heating and Cooling Energy System Planning in Arid Climates. *Energy*, **218**, Article ID: 119421. https://doi.org/10.1016/j.energy.2020.119421

[2] Simões, N., Manaia, M. and Simões, I. (2021) Energy Performance of Solar and Trombe Walls in Mediterranean Climates. *Energy*, **234**, Article ID: 121197. https://doi.org/10.1016/j.energy.2021.121197

[3] Khedari, J., Boonsri, B. and Hirunlabh, J. (2000) Ventilation Impact of a Solar Chimney on Indoor Temperature Fluctuation and Air Change in a School Building. *Energy and Buildings*, **32**, 89-93. https://doi.org/10.1016/s0378-7788(99)00042-0

[4] Pourshab, N., Tehrani, M.D., Toghraie, D. and Rostami, S. (2020) Application of Double Glazed Façades with Horizontal and Vertical Louvers to Increase Natural Air Flow in Office Buildings. *Energy*, **200**, Article ID: 117486. https://doi.org/10.1016/j.energy.2020.117486

[5] Monghasemi, N. and Vadiee, A. (2017) A Review of Solar Chimney Integrated Systems for Space Heating and Cooling Application. *Renewable and Sustainable Energy Reviews*, **81**, 2714-2730.

[6] Jafari, A. and Haghighi Poshtiri, A. (2017) Passive Solar Cooling of Single-Storey Buildings by an Adsorption Chiller System Combined with a Solar Chimney. *Journal of Cleaner Production*, **141**, 662-682. https://doi.org/10.1016/j.jclepro.2016.09.099

[7] Zhang, T., Tan, Y., Yang, H. and Zhang, X. (2016) The Application of Air Layers in Building Envelopes: A Review. *Applied Energy*, **165**, 707-734. https://doi.org/10.1016/j.apenergy.2015.12.108

[8] Zhang, H., Yang, D., Tam, V.W.Y., Tao, Y., Zhang, G., Setunge, S., *et al.* (2021) A Critical Review of Combined Natural Ventilation Techniques in Sustainable Buildings. *Renewable and Sustainable Energy Reviews*, **141**, Article ID: 110795. https://doi.org/10.1016/j.rser.2021.110795

[9] Harris, D.J. and Helwig, N. (2007) Solar Chimney and Building Ventilation. *Applied Energy*, **84**, 135-146. https://doi.org/10.1016/j.apenergy.2006.07.001

[10] Khanal, R. and Lei, C. (2011) Solar Chimney—A Passive Strategy for Natural Ventilation. *Energy and Buildings*, **43**, 1811-1819. https://doi.org/10.1016/j.enbuild.2011.03.035

[11] Chungloo, S. and Limmeechokchai, B. (2009) Utilization of Cool Ceiling with Roof Solar Chimney in Thailand: the Experimental and Numerical Analysis. *Renewable Energy*, **34**, 623-633. https://doi.org/10.1016/j.renene.2008.05.026

[12] Sudprasert, S., Chinsorranant, C. and Rattanadecho, P. (2016) Numerical Study of Vertical Solar Chimneys with Moist Air in a Hot and Humid Climate. *International Journal of Heat and Mass Transfer*, **102**, 645-656. https://doi.org/10.1016/j.ijheatmasstransfer.2016.06.054

[13] Gan, G. and Riffat, S.B. (1998) A Numerical Study of Solar Chimney for Natural Ventilation of Buildings with Heat Recovery. *Applied Thermal Engineering*, **18**, 1171-1187. https://doi.org/10.1016/s1359-4311(97)00117-8

[14] Mathur, J., Mathur, S. and Anupma (2006) Summer-Performance of Inclined Roof Solar Chimney for Natural Ventilation. *Energy and Buildings*, **38**, 1156-1163. https://doi.org/10.1016/j.enbuild.2006.01.006

[15] Khanal, R. and Lei, C. (2014) An Experimental Investigation of an Inclined Passive Wall Solar Chimney for Natural Ventilation. *Solar Energy*, **107**, 461-474. https://doi.org/10.1016/j.solener.2014.05.032

[16] Sakonidou, E.P., Karapantsios, T.D., Balouktsis, A.I. and Chassapis, D. (2008) Modeling of the Optimum Tilt of a Solar Chimney for Maximum Air Flow. *Solar Energy*, **82**, 80-94. https://doi.org/10.1016/j.solener.2007.03.001

[17] Gan, G. (1998) A Parametric Study of Trombe Walls for Passive Cooling of Buildings. *Energy and Buildings*, **27**, 37-43. https://doi.org/10.1016/s0378-7788(97)00024-8

[18] Onbasioglu, H. and Egrican, A.N. (2002) Experimental Approach to the Thermal Response of Passive Systems. *Energy Conversion and Management*, **43**, 2053-2065. https://doi.org/10.1016/s0196-8904(01)00138-8

[19] Gan, G. (2006) Simulation of Buoyancy-Induced Flow in Open Cavities for Natural Ventilation. *Energy and Buildings*, **38**, 410-420. https://doi.org/10.1016/j.enbuild.2005.08.002

[20] Arce, J., Jiménez, M.J., Guzmán, J.D., Heras, M.R., Alvarez, G. and Xamán, J. (2009) Experimental Study for Natural Ventilation on a Solar Chimney. *Renewable Energy*, **34**, 2928-2934. https://doi.org/10.1016/j.renene.2009.04.026

[21] Asadi, S., Fakhari, M., Fayaz, R. and Mahdaviparsa, A. (2016) The Effect of Solar Chimney Layout on Ventilation Rate in Buildings. *Energy and Buildings*, **123**, 71-78. https://doi.org/10.1016/j.enbuild.2016.04.047

[22] Ong, K.S. (2003) A Mathematical Model of a Solar Chimney. *Renewable Energy*, **28**, 1047-1060. https://doi.org/10.1016/s0960-1481(02)00057-5

[23] Hirunlabh, J., Kongduang, W., Namprakai, P. and Khedari, J. (1999) Study of Natural Ventilation of Houses by a Metallic Solar Wall under Tropical Climate. *Renewable Energy*, **18**, 109-119. https://doi.org/10.1016/s0960-1481(98)00783-6

[24] Bansal, N.K., Mathur, J., Mathur, S. and Jain, M. (2005) Modeling of Window-Sized Solar Chimneys for Ventilation. *Building and Environment*, **40**, 1302-1308. https://doi.org/10.1016/j.buildenv.2004.10.011

[25] Miyazaki, T., Akisawa, A. and Kashiwagi, T. (2006) The Effects of Solar Chimneys on Thermal Load Mitigation of Office Buildings Under the Japanese Climate. *Renewable Energy*, **31**, 987-1010. https://doi.org/10.1016/j.renene.2005.05.003

[26] Zamora, B. and Kaiser, A.S. (2009) Optimum Wall-to-wall Spacing in Solar Chimney Shaped Channels in Natural Convection by Numerical Investigation. *Applied Thermal Engineering*, **29**, 762-769. https://doi.org/10.1016/j.applthermaleng.2008.04.010

[27] da Silva, A.K. and Gosselin, L. (2005) Optimal Geometry of L and C-Shaped Channels for Maximum Heat Transfer Rate in Natural Convection. *International Journal of Heat and Mass Transfer*, **48**, 609-620. https://doi.org/10.1016/j.ijheatmasstransfer.2004.08.028

[28] Neves, L., Roriz, M. and Marques, F. (2011) Modeling a Solar Chimney for Maxi-Mum Solar Irradiation and Maximum Airflow, for Low Latitude Locations. *Prceedings of the* 12*th Conference of the International Building Performance Simulation Association*, Sydney, 14-16 November 2011, 14-16.

[29] Kumar, L.M., Sivaramakrishnan, V., Premalatha, M. and Vivekanandan, M. (2016) Interpretation on Result of Directions of Suction Opening on Solar Chimney Coherent with Building. *Journal of Scientific & Industrial Research*, **75**, 194-199.

[30] Imran, A.A., Jalil, J.M. and Ahmed, S.T. (2015) Induced Flow for Ventilation and Cooling by a Solar Chimney. *Renewable Energy*, **78**, 236-244. https://doi.org/10.1016/j.renene.2015.01.019

[31] Charvat, P., Jicha, M. and Stetina, J. (2014) Solar Chimneys for Ventilation and Pas-

sive Cooling. https://www.researchgate.net/publication/264882993

[32] Chungloo, S. and Limmeechokchai, B. (2007) Application of Passive Cooling Systems in the Hot and Humid Climate: The Case Study of Solar Chimney and Wetted Roof in Thailand. *Building and Environment*, **42**, 3341-3351. https://doi.org/10.1016/j.buildenv.2006.08.030

[33] Bachrun, A.S., Ming, T.Z. and Kurniasih, S. (2020) Building's Solar Chimney: Ambient Obstacle and Crosswind in a Tropical Country. In: Ming, T.Z. and Kurniasih, S., Eds., *Proceedings of the EduARCHsia & Senvar* 2019 *International Conference* (*EduARCHsia* 2019), Atlantis Press, Amsterdam, 53-60. https://doi.org/10.2991/aer.k.200214.008

[34] Daho, T. and Tubreoumya, G. C. (2019) Modelisation des paramètres de fonctionnement d'un Cuiseur Solaire de type Boîte sous les Conditions Météorologiques du Burkina Faso. *Journal de Physique de la SOAPHYS*, **1**, 1-8. https://www.soaphys.org/wp-content/uploads/2020/02/Nebie.pdf

[35] Boukaré, O., Boureima, K., Germain, O.W.P., Kalifa, P. and Bahiebo, D.J. (2024) Practical Exploration of the "Open or Close" Concept: Evaluation of the Hygrothermal Performance of a Bioclimatic Innovation for Onion Bulb Preservation. *Advanced Engineering Forum*.

[36] Afonso, C. and Oliveira, A. (2000) Solar Chimneys: Simulation and Experiment. *Energy and Buildings*, **32**, 71-79. https://doi.org/10.1016/s0378-7788(99)00038-9

[37] Sandberg, M. (1999) Cooling of Building Integrated Photovoltaics by Ventilation Air. *Air Infiltration and Ventilation Centre*, **12**, Article No. 533. https://www.aivc.org/sites/default/files/airbase_12533.pdf

[38] Sandberg, M. and Moshfegh, B. (1998) Ventilated-Solar Roof Air Flow and Heat Transfer Investigation. *Renewable Energy*, **15**, 287-292. https://doi.org/10.1016/s0960-1481(98)00175-x

[39] Shi, L. and Zhang, G. (2016) An Empirical Model to Predict the Performance of Typical Solar Chimneys Considering Both Room and Cavity Configurations. *Building and Environment*, **103**, 250-261. https://doi.org/10.1016/j.buildenv.2016.04.024

[40] Bacharoudis, E., Vrachopoulos, M.G., Koukou, M.K., Margaris, D., Filios, A.E. and Mavrommatis, S.A. (2007) Study of the Natural Convection Phenomena Inside a Wall Solar Chimney with One Wall Adiabatic and One Wall under a Heat Flux. *Applied Thermal Engineering*, **27**, 2266-2275. https://doi.org/10.1016/j.applthermaleng.2007.01.021